Video Article

Experimental Investigation of the Flow Structure over a Delta Wing Via Flow Visualization Methods

Lu Shen[1], Zong-nan Chen[1], Chihyung Wen[1]

[1]Department of Mechanical Engineering, Hong Kong Polytechnic University

Correspondence to: Chihyung Wen at cywen@polyu.edu.hk

URL: https://www.jove.com/video/57244
DOI: doi:10.3791/57244

Keywords: Engineering, Issue 134, Delta Wing, Smoke Flow Visualization, Leading Edge Vortex, Vortex Breakdown, Vortex Oscillation, Particle Image Velocimetry

Date Published: 4/23/2018

Citation: Shen, L., Chen, Z.n., Wen, C. Experimental Investigation of the Flow Structure over a Delta Wing Via Flow Visualization Methods. *J. Vis. Exp.* (134), e57244, doi:10.3791/57244 (2018).

Abstract

It is well known that the flow field over a delta wing is dominated by a pair of counter rotating leading edge vortices (LEV). However, their mechanism is not well understood. The flow visualization technique is a promising non-intrusive method to illustrate the complex flow field spatially and temporally. A basic flow visualization setup consists of a high-powered laser and optic lenses to generate the laser sheet, a camera, a tracer particle generator, and a data processor. The wind tunnel setup, the specifications of devices involved, and the corresponding parameter settings are dependent on the flow features to be obtained.

Normal smoke wire flow visualization uses a smoke wire to demonstrate the flow streaklines. However, the performance of this method is limited by poor spatial resolution when it is conducted in a complex flow field. Therefore, an improved smoke flow visualization technique has been developed. This technique illustrates the large-scale global LEV flow field and the small-scale shear layer flow structure at the same time, providing a valuable reference for later detailed particle image velocimetry (PIV) measurement.

In this paper, the application of the improved smoke flow visualization and PIV measurement to study the unsteady flow phenomena over a delta wing is demonstrated. The procedure and cautions for conducting the experiment are listed, including wind tunnel setup, data acquisition, and data processing. The representative results show that these two flow visualization methods are effective techniques for investigating the three-dimensional flow field qualitatively and quantitatively.

Video Link

The video component of this article can be found at https://www.jove.com/video/57244/

Introduction

Flow field measurement via visualization techniques is a basic methodology in fluid engineering. Among the different visualization techniques, smoke wire flow visualization in wind tunnel experiments and dye visualization in water tunnel experiments are the most widely used to illustrate flow structures qualitatively. PIV and laser Doppler anemometry (LDA) are two typical quantitative techniques[1].

In smoke wire flow visualization, smoke streaklines are generated from oil droplets on a heating wire or injected from the outer smoke generator/container during the experiments. High-power lights or laser sheets are used to illuminate the smoke streaklines. Images are then recorded for further analysis. This is a simple but very useful flow visualization method[2]. However, the effectiveness of this method may be limited by various factors, such as the short duration of smoke wires, the complex three-dimensional flow field, the relatively high velocity of the flow, and the efficiency of smoke generation[3].

In PIV measurements, a cross-section of a flow field with entrained particles is illuminated by a laser sheet, and instant positions of the particles in this cross-section are captured by a high-speed camera. Within an extremely small time interval, a pair of images is recorded. By dividing the images into a grid of interrogation areas and calculating the average motion of particles in interrogation areas through cross-correlation functions, the instantaneous velocity vector map in this observed cross-section can be obtained. However, it is also known that compromises must be reached for factors including the size of the observation window, the resolution of the velocity map, the velocity magnitude in the plane, the time interval between the pair of images, the orthogonal velocity magnitude, and the particle density[4]. Therefore, many exploratory experiments may be needed to optimize the experimental settings. It would be expensive and time-consuming to investigate an unknown and complex flow field with PIV measurement alone[5,6]. Considering the above concerns, a strategy to combine smoke flow visualization and PIV measurement is proposed and demonstrated here to study the complex flow over a slender delta wing.

Numerous studies of LEV flows over delta wings have been conducted[7,8], with flow visualization techniques used as the primary tools. Many interesting flow phenomena have been observed: spiral type and bubble type vortex breakdowns[9,10], an unsteady shear layer substructure[11,12], oscillations of LEV breakdown locations[13], and effects of pitching and yaw angles[14,15,16] on the flow structures. However, the underlying mechanisms of some unsteady phenomena in the delta wing flows remain unclear[7]. In this work, the smoke flow visualization is improved

Copyright © 2018 Journal of Visualized Experiments

using the same seeding particles used in PIV measurement, instead of a smoke wire. This improvement greatly simplifies the operation of the visualization and increases the quality of the images. Based on the results from the improved smoke flow visualization, PIV measurement focuses on those flow fields of interest to acquire the quantitative information.

Here, a detailed description is provided to explain how to conduct a flow visualization experiment in a wind tunnel and to investigate unsteady flow phenomena over a delta wing. Two visualization methods, the improved smoke flow visualization and PIV measurement, are used together in this experiment. The procedure includes step-by-step guidance for device setup and parameter adjustment. Typical results are demonstrated to show the advantage of combining these two methods for measuring the complex flow field spatially and temporally.

Protocol

1. Wind Tunnel Setup

1. **Delta wing model**
    1. Construct a delta wing model from aluminum, with a sweep angle φ of 75°, a chord length c of 280 mm, a root span b of 150 mm, and a thickness of 5 mm. Have both leading edges beveled at 35° to fix the separation point[17] (see **Figure 1a**).

2. **Wind tunnel facility**
    1. Conduct experiments in a closed-loop low-speed wind tunnel, with a test section of 2.4 m (length) × 0.6 m (width) × 0.6 m (height) that is equipped with glass walls that allow optical access during the experiments. The turbulent intensity of such a facility should be less than 0.4%.
    NOTE: In this study, we used a wind tunnel at The Hong Kong Polytechnic University with the above characteristics. Also, the freestream velocity U_∞ ranged from 2.64 m/s to 10.56 m/s, corresponding to a Reynolds number, Re, from 5×10^4 to 2×10^5, based on the chord length of the delta wing, which is the typical flight range for an unmanned aerial vehicle (UAV).
    2. As needed, use three different arrangements (see **Figure 1b**-d) of the laser sheet and the cameras to observe the flow structures in the longitudinal cross section, the span-wise cross section, and the transverse cross section. Schematics of the setup are shown in **Figure 1b**.
    NOTE: This protocol demonstrates the setup and measurement in the longitudinal cross section in detail.

3. **Install the delta wing**
    1. Fix the delta wing trailing edge on the sting, which is on a circular motion guide used for adjusting the angle of attack (AoA), α. The center of the circular guide is on the central line of the wind tunnel test section. Thus, the delta wing's center can always be at the center of the test section. Adjust the AoA to α = 34°.
    2. Carefully adjust the delta wing model to minimize any yaw angle and roll angle, by checking the readings of an angle meter and a three-axis laser level. In the current study, the uncertainty of these two angles is less than 0.1°.

4. **Set up the laser sheet**
    1. Use two lasers separately to illuminate the flow structures for PIV measurement and smoke flow visualization.
        1. For PIV measurement, use a dual pulse laser, with a wavelength of 532 nm and a maximum energy of 600 mJ (adjustable) for each pulse. Control it with a synchronizer with transistor-transistor logic (TTL) signals (see **Figure 1b**).
        2. For smoke flow visualization, use a continuous laser with a wavelength of 532 nm and a power of 1 W. This continuous laser works independently. During the setup installation, use a neutral density filter with 10% transmittance to filter the laser beam for safety.
    2. Wear appropriate laser goggles.
    3. Adjust the reflection mirror to introduce the laser beam into the wind tunnel. The angle between the laser light axis and the mirror is $\frac{1}{2}(90° - \alpha) = 28°$, to make the laser beam normal to the delta wing surface. Ensure that the laser beam is around the position x/c # 0.25, which will later be the center of the field of view (FOV).
    4. Install laser optics (with the continuous laser, at first) to form the laser sheet, as shown in **Figure 1b**. The convex lens is used to control the laser beam size (also the sheet thickness). The cylindrical lens expands the laser beam to a laser sheet.
    NOTE: In the current study, the focal length of the cylindrical lens is 700 mm, and the diameter of the cylindrical lens is 12 mm.
    5. Check the laser sheet thickness by measuring the laser line on the model. Adjust the location of the convex lens if the laser sheet thickness is not suitable (here, around 1 mm, with an effective width of the laser sheet in the test section of about 100 mm). Note that the thickness of the laser sheet is dependent on 1) the velocity component in the normal direction to the laser sheet and 2) the time interval between the pair of snapshots in PIV measurement.
    6. Put a calibration target plate on the delta wing, with its surface coincident to the laser sheet. This step is essential because the FOV in the current study is not orthogonal to the wind tunnel coordinate.

5. **Camera setup**
    1. Turn off the lasers when setting up the camera. As with the lasers, use two cameras for each separate part of this experiment:
        1. For PIV measurement, use a high-speed CCD camera with a resolution of 2048 × 2048 pixels. This camera is controlled by the synchronizer and the dual pulse laser (see **Figure 1b**). Data in this camera will be transmitted directly to the computer.
        2. For smoke flow visualization, use a commercial digital camera with a snapshot resolution of 4,000 × 6,000 pixels and a 50 Hz video recording resolution of 720 × 1280 pixels during the smoke flow visualization. It will be operated manually.
    2. Move the camera's position (commercial digital camera, at first) to obtain the desired FOV. Adjust the camera lens to focus on the calibration target plate. Make sure the entire field is focused. If not, the coordinates of the camera may not be orthogonal to the calibration target plate. Thus, adjust the camera's position carefully[18].

3. Take several frames after the camera is well set. Later, these frames of the calibration target plate will be used to calibrate the scale factor between the real size and the frame pixel, and to identify the reference position in the xyz coordinate. Then, remove the calibration target plate.

6. Turn on the wind tunnel at a low speed (*e.g.*, 3 m/s) and inject oil particles into the wind tunnel. Set the pressure of the aerosol generator at 2.5 bar and operate it for 30 s for the pre-seeded flow visualization method. After this, the whole wind tunnel will be uniformly seeded with oil particles at a normal diameter of about 1 µm.
   NOTE: In the current study, the estimated oil particle density concentration in the wind tunnel is approximately $650\ \mu g/m^3$ in the smoke flow visualization; thus, the overall flow density change in the wind tunnel is $\frac{\rho' - \rho}{\rho} < 0.1\%$.
7. **PIV software setup**
   1. Control the PIV system with the PIV software (see Table of Materials). This software can command the synchronizer to send TTL signals to the laser and the camera, as shown in **Figure 1b**.
   2. Set the sampling frequency at 5 Hz, with a total sampling number of 500. The time interval between PIV frames is 80 µs. Note that the time interval is dependent on the size of the FOV and flow velocity. Make sure that the interrogation areas in two frames have about a 50 - 75% overlap.

2. Running the Experiment

1. **Improved smoke flow visualization**
   1. Turn on the wind tunnel at the desired freestream velocity (U = 2.64 m/s). Run it for 10 min to stabilize the freestream velocity. At Re = 50,000, the freestream velocity is U = 2.64 m/s.
   2. Turn on the continuous laser. Use the digital camera to capture 5 - 10 snapshots of the flow structure.
   3. Check whether the laser sheet is at the longitudinal cross-section of the LEV core (see the typical structure shown in **Figure 3**). If so, mark this position on the delta wing model as a reference for the later PIV measurement; otherwise, change the position of the laser sheet by adjusting the optic lens and reset the calibration following steps 1.4.6 - 1.5.3.
   4. Review those images and check the focus and brightness. If the image quality is not satisfactory, adjust the aperture of the lens or the ISO setup.
   5. Take more snapshots (typically around 20) and videos (approximately 40 s) with the proper setup. Turn off the laser and transfer the data to the computer.

2. **PIV measurement**
   1. Based on the reference position known from step 2.1.3 and the results of the snapshots from step 2.1.5, choose an interesting region ($x/c \approx 0.3$) as the FOV, where vortical substructures can be observed. Replace the continuous laser and digital camera with the dual pulse laser and CCD camera for PIV measurement.
   2. Repeat steps 1.4.6 - 1.5.3 to record the calibration for PIV measurement.
   3. Turn on the wind tunnel at the desired freestream velocity, U = 2.64 m/s. Run it for 10 minutes to ensure that the freestream velocity is stable.
   4. Adjust the dual pulse laser to the highest power level and stand by. Use the software to start the data acquisition for 100 s. Once the data recording has finished, turn off the laser head.
   5. Review the acquired images in the software and check the laser sheet distribution, the particle density (usually 6-10 particles in each desired interrogation area), the focus, and the particle displacement between the double frames (25-50% of the interrogation area).
   6. If the quality of the images is satisfactory, as described in step 2.2.5., save the data onto the hard disk of the PC and run the other cases by repeating the above steps. Otherwise, repeat steps 1.7 and 2.2 and carefully adjust the setup.

3. Data Processing

1. **Improved smoke visualization**
   NOTE: The following steps, 3.1.1-3.1.4, are done via MATLAB code automatically (see the **Supplemental Coding File**).
   1. Transform the video into a sequence of frames. Convert the frames from the RGB form into grayscale. Rotate the frame to make the delta wing surface horizontal. Choose the area of interest for later processing (**Figure 2a**).
   2. Adjust the brightness and the contrast to highlight the flow structure. Apply an adaptive threshold to transform the gray image to a binary image (**Figure 2b**).
   3. Add up the binary values in each column and find the position at which the sum suddenly changes. This position is the vortex breakdown location (**Figure 2c**).
   4. Record the vortex breakdown locations and their corresponding times. The time history of the breakdown oscillation thus can be obtained.
   5. Use the pixel-real size scale factor (measured from the images with the calibration target plate in step 1.5.3) to transform the time history from pixels to real size and to identify the reference position. Plot the time history of the breakdown oscillation.

2. **PIV measurement**
   1. Run the PIV software. Use the images acquired in step 2.2.2 to set the scale factor and the reference position of the coordinates. Pre-process the acquired data through the image processing library to highlight the particles and reduce noise[18].
   2. Use the adaptive interrogation area method with a minimum grid size of 32 × 32 pixels and a minimum overlap of 50%. Choose the image area and set a 3 x 3 vector validation for the adaptive cross-correlations.

3. The result is given as a velocity vector field, in which the blue vectors are the correct vectors, the green ones are the substituted vectors, and the red ones are bad vectors.
4. Apply the 3 x 3 moving average validation method to estimate the local velocity by comparing the vectors in its neighborhood. Replace vectors that deviate too much from their neighbors with the average of their neighbors.
5. Calculate vector statistics in the velocity maps to obtain the flow characteristics in the time history, *e.g.*, the time-averaged velocity, the standard deviation, and the cross-correlation between velocity components. Compute the scalar derivatives from the vector map to demonstrate the internal features of the flow field, *e.g.*, the vorticity, shear stresses, and swirling strength.

Representative Results

Figure 2d shows the time histories of the LEV breakdown locations. The black curve indicates the portside LEV and the red curve indicates the starboard LEV. The time scale is nondimensionalized by the free stream velocity and chord length. The correlation coefficient between these two time histories is $r = -0.53$, indicating a strong anti-symmetric interaction of the LEV breakdown location oscillations. This result agrees well with the work of others[13,19,20].

Figure 3 shows the LEV flow structure in the longitudinal cross section at $\alpha = 34°$ and $Re = 75{,}000$. The original image was captured by the digital camera in RGB form, with an exposure duration of 1/500 seconds. In this figure, the coordinate is normalized by the delta wing chord length. A 10 mm scale is plotted at the upper right corner for reference. The result clearly demonstrates the primary LEV core, which develops from the tip of the delta wing to the downstream in a straight line. Near the position at $x = 0.19\ c$, the vortex core suddenly expands. This is known as the leading edge vortex breakdown[9,21]. After the breakdown location, the wake becomes turbulent. Around the primary LEV core are small vortical structures. These substructures originate from the leading edges and swirl around the primary vortex core within the rolling up shear layer[12,22,23]. As the substructures move into the inner layer of the LEV, their shape is stretched due to the relatively high velocity component in the longitudinal direction near the vortex core. During the experiment, it is noted that the flow structure of the LEV is quite stationary, except at the LEV breakdown location. This result shows that this smoke flow visualization method can achieve a good balance between the local small flow structure and the global flow structure evolution.

Figure 4 shows the typical particle images in a 64 x 64 pixel region, captured from PIV measurement. In the 32 x 32 pixel interrogation area in Frame A, there are 10 identified particles, marked by yellow circles. After the time interval between two frames, these particles displace to new locations, as shown in Frame B. The displacements are about one-quarter of the interrogation area, resulting in an almost 70% overlap between these interrogation areas. Additionally, almost all of the particles remain in the laser sheet plane, indicating that the setup parameters were appropriately chosen for this case.

Figure 5 shows the time-averaged PIV results in the streamwise and spanwise cross sections. Before these measurements are carried out, the improved smoke flow visualization is conducted to identify the primary vortex core position, following steps 2.1.1 - 2.1.3. The coordinates in **Figure 5** are normalized by the delta wing chord length c and the local semispan length S_L. The vorticity ω is normalized as $\omega^* = \omega U_\infty / c$. According to this result, the primary vortex core can be easily identified by the inflection line of the positive and negative vorticities, and it is marked by the black dotted line. In the upper and bottom regions, the rolling shear layers show large vorticities. The λ_{ci} criterion[24,25] is used to identify the vortices from PIV measurement. In **Figure 5**, the solid lines illustrate the region with a local swirling strength lower than zero, indicating the existence of vortices. Near the core, the substructures are stretched and do not appear in the swirling strength contour. However, the concentrated vorticity contour still suggests the substructures here, marked by the white dotted line. In **Figure 5b**, the velocity vector map clearly illustrates that on each side, the flow separates at the leading edge and forms a strong shear layer, which later rolls into the LEV core. Complementary to the flow structure in the streamwise cross section, the spanwise flow structure clearly shows the evolution of the outer vortical substructures.

Copyright © 2018 Journal of Visualized Experiments

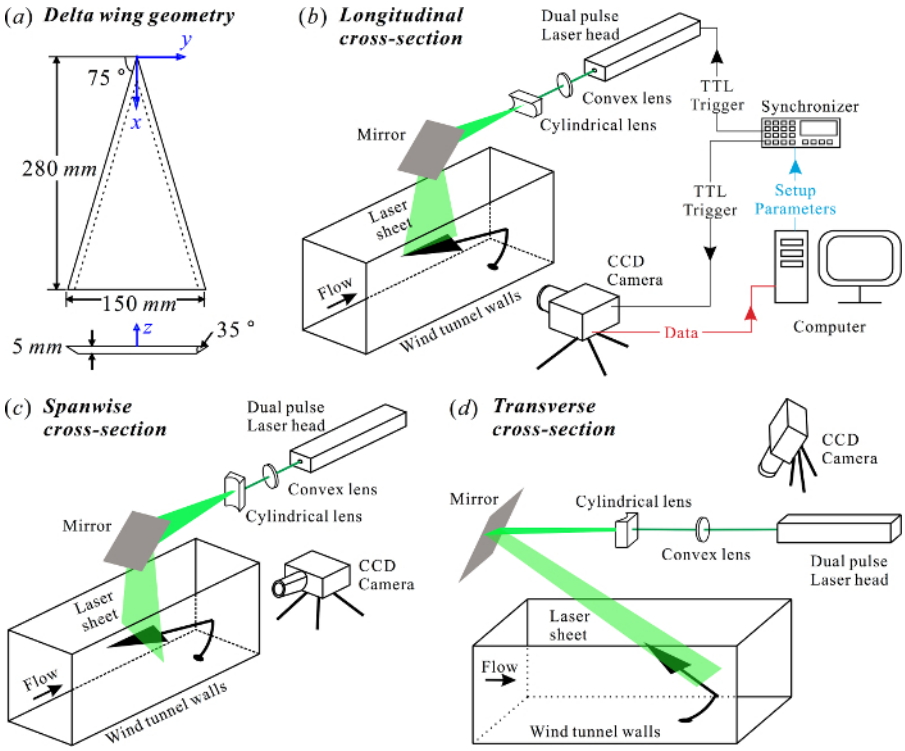

Figure 1: Schematics of setups. (a) The delta wing model; **(b-d)** setups for PIV measurement in the longitudinal cross-section, the spanwise cross-section, and the transverse cross-section, respectively. Please click here to view a larger version of this figure.

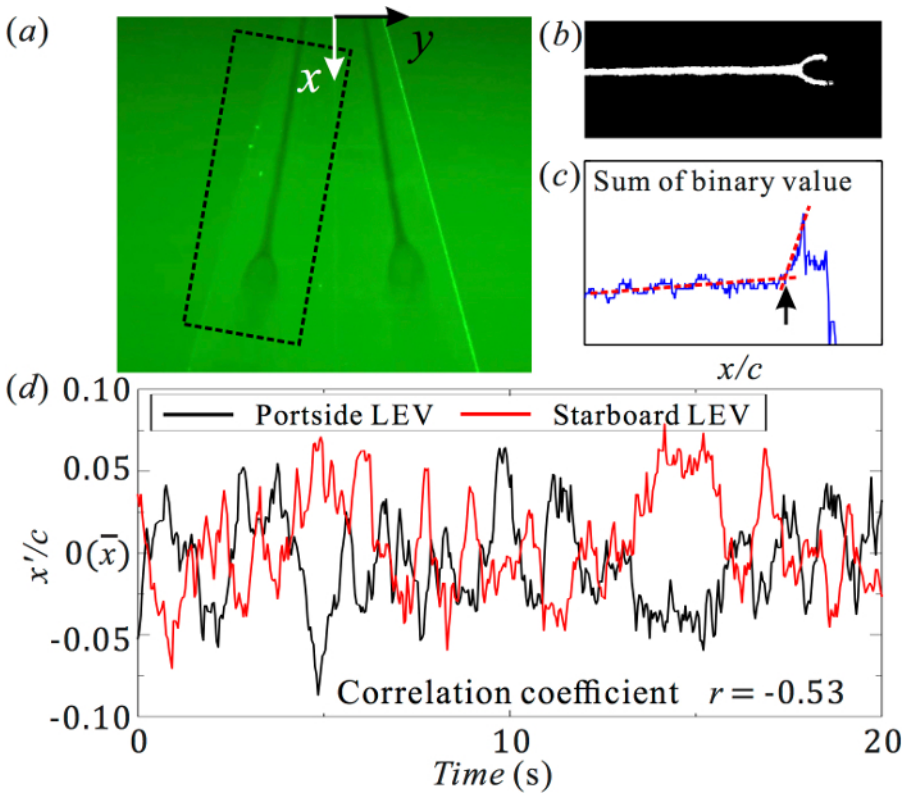

Figure 2: Measurement of the LEV breakdown location. (a) A smoke flow visualization result showing the leading-edge vortex structure in the transverse cross section: α = 34° and *Re* = 50,000; the marked area is rotated and further processed. **(b)** The binary image of the marked area in (a), clearly showing the LEV core and breakdown. **(c)** The summation of each column in the binary image (b) and the identified LEV breakdown location in the streamwise direction (x-direction), normalized by the chord length *c*. **(d)** The time histories of the LEV breakdown locations. $\bar{x}$ is the time-averaged position and x' is the instant distance to the time-averaged position. Please click here to view a larger version of this figure.

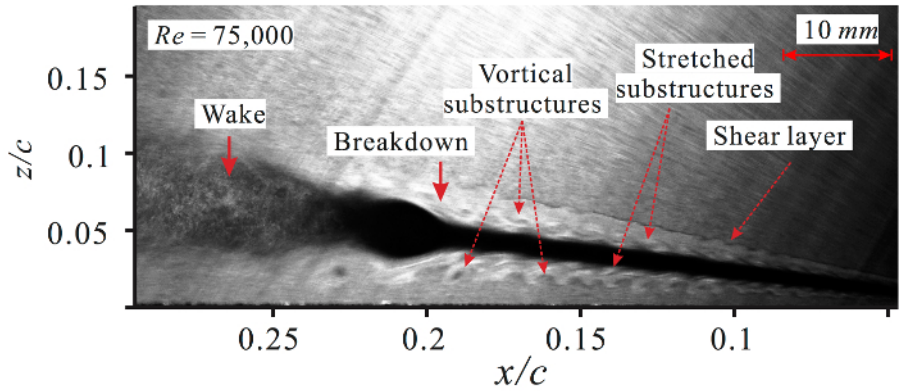

Figure 3: The leading-edge vortex structure in the longitudinal cross section at α = 34° and *Re* = 75,000, obtained from the smoke flow visualization. Please click here to view a larger version of this figure.

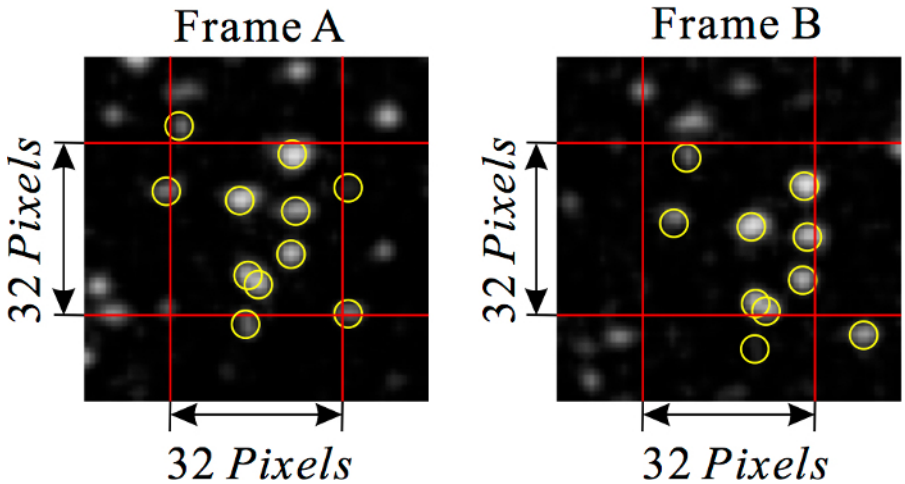

Figure 4: Particle images in a 64 x 64 pixel region. The corresponding interrogation area is 32 x 32 pixels. The time interval between Frames A and B is 80 microseconds. The identified particles in the original interrogation area are marked by yellow circles. Please click here to view a larger version of this figure.

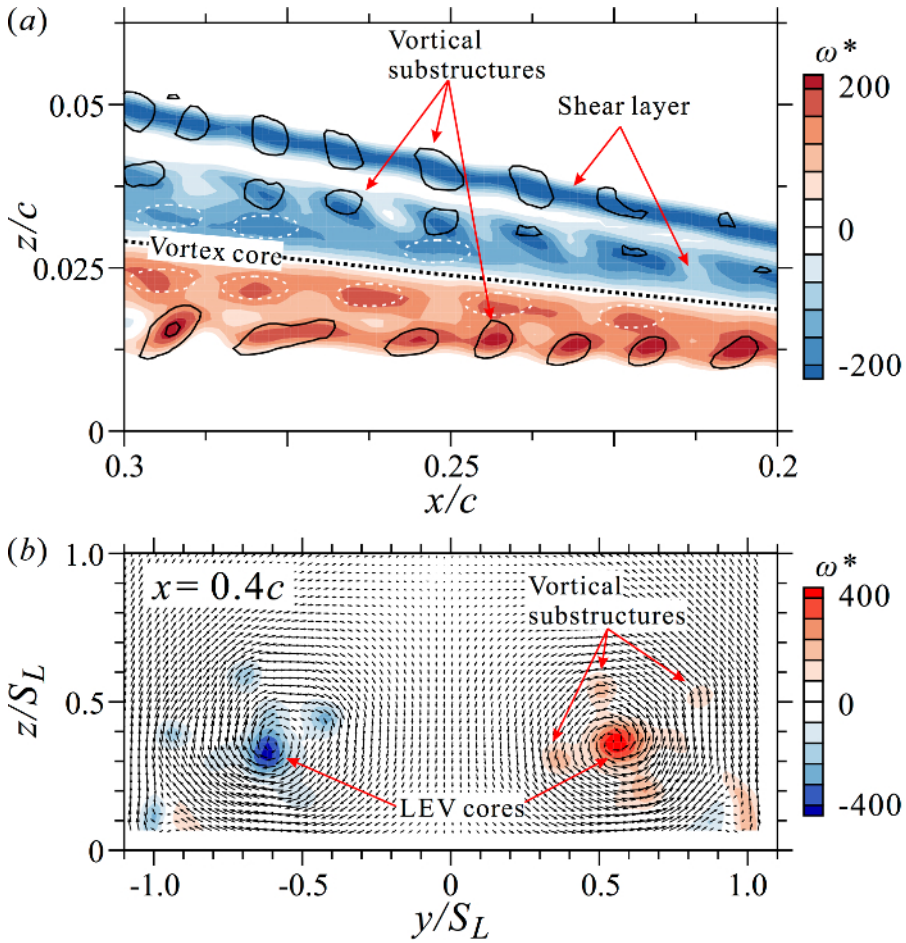

Figure 5: Time-averaged PIV results. (**a**) Dimensionless vorticity ω^* contour with solid lines marking the regions with local swirling strength lower than zero in the longitudinal cross section. (**b**) Dimensionless vorticity ω^* contour with velocity vectors in the spanwise cross section at x = 0.4c; coordinates are normalized by the local semispan length S_L (α = 34° and Re = 50,000). Please click here to view a larger version of this figure.

Discussion

This article presents the two flow visualization methods, improved smoke flow visualization and PIV measurement, to investigate flow structure over the delta wing qualitatively and quantitatively. The general procedures of the experiment are described step by step. The setups of these two methods are almost the same, while the devices involved are different. The basic principle of these two flow visualization methods is to illuminate the particles in the flow via the laser sheet. The improved smoke flow visualization can obtain the global flow structure and small local structures at the same time, which is helpful for obtaining an overview of an unknown flow structure. The quantitative PIV analysis provides a detailed vector map of the interesting flow field. Thus, combining these flow visualization methods can significantly improve research efficiency.

Compared with normal smoke wire flow visualization, the smoke flow visualization method demonstrated here is rather efficiently conducted. Because the particles are uniformly distributed, small flow structures are easily identified. In a complex three-dimensional flow, this method allows the laser sheet to be set up at any spatial position to observe the flow fields in different cross-sections, whereas in the traditional smoke wire method, the laser sheet must always be aligned with the smoke direction and the observation window is accordingly limited[26]. Additionally, this improved method should not miss any flow details caused by the absence of the smoke in some regions during a smoke wire experiment. However, this method would not be suitable for open-loop wind tunnel facilities due to how seeding is conducted. Flow visualization data should be carefully analyzed to avoid the pitfalls of imaginary illuminations[3,27].

Because the flow field over the delta wing is highly three-dimensional and sensitive to any disturbance, non-intrusive investigations are recommended[21]. For measurements in planes, it is essential to consider the orthogonal velocity component on the observation plane during PIV measurement[28,29]. In this case, the time interval between two frames and the laser sheet thickness should be a compromise with the orthogonal velocity to ensure that most of the particles do not move out the laser sheet. For similar measurements, it is suggested to run several cases with different setup parameters in advance to identify the most suitable ones.

The flow visualization methods described in this paper are convenient, efficient, and low-cost. In the future, these techniques will be applied to complex flow fields with active flow control, such as bluff body drag reduction and vortex-structure interaction, to evaluate control effects quickly, understand control mechanisms, and accelerate the optimization of control parameters.

Copyright © 2018 Journal of Visualized Experiments

Disclosures

The authors have nothing to disclose.

Acknowledgements

The authors would like to thank Hong Kong Research Grants Council (no. GRF526913), Hong Kong Innovation and Technology Commission (no. ITS/334/15FP), and the US Office of Naval Research Global (no. N00014-16-1-2161) for financial support.

References

1. Smits, A. J. *Flow visualization: Techniques and examples.* World Scientific (2012).
2. Barlow, J. B., Rae, W. H., & Pope, A. *Low-speed wind tunnel testing.* New York: Wiley (1999).
3. Merzkirch, W. *Flow visualization.* Academic Press, inc. (1987).
4. Raffel, M., Willert, C. E., Wereley, S., & Kompenhans, J. *Particle image velocimetry: A practical guide.* Springer (2007).
5. Westerweel, J., Elsinga, G. E., & Adrian, R. J. Particle Image Velocimetry for Complex and Turbulent Flows. *Annu Rev Fluid Mech.* **45** (1), 409-436 (2013).
6. Meinhart, C. D., Wereley, S. T., & Santiago, J. G. PIV measurements of a microchannel flow. *Exp Fluids.* **27** (5), 414-419 (1999).
7. Gursul, I. Review of unsteady vortex flows over slender delta wings. *J Aircraft.* **42** (2), 299-319 (2005).
8. Gursul, I., Gordnier, R., & Visbal, M. Unsteady aerodynamics of nonslender delta wings. *Prog Aerosp Sci.* **41** (7), 515-557 (2005).
9. Lowson, M. Some experiments with vortex breakdown. *JRoy Aeronaut Soc.* **68,** 343-346, (1964).
10. Payne, F. M., Ng, T., Nelson, R. C., & Schiff, L. B. Visualization and wake surveys of vortical flow over a delta wing. *AIAA J.* **26** (2), 137-143 (1988).
11. Lowson, M. V. The three dimensional vortex sheet structure on delta wings. *Fluid Dynamics of Three-Dimensional Turbulent Shear Flows and Transition.* 11.11-11.16 (1989).
12. Riley, A. J., & Lowson, M. V. Development of a three-dimensional free shear layer. *J Fluid Mech.* **369,** 49-89, (1998).
13. Menke, M., & Gursul, I. Unsteady nature of leading edge vortices. *Phys Fluids.* **9** (10), 2960 (1997).
14. Yayla, S., Canpolat, C., Sahin, B., & Akilli, H. Yaw angle effect on flow structure over the nonslender diamond wing. *AIAA J.* **48** (10), 2457-2461 (2010).
15. Menke, M., & Gursul, I. Nonlinear response of vortex breakdown over a pitching delta Wing. *J Aircraft.* **36** (3), 496-500 (1999).
16. Sahin, B., Yayla, S., Canpolat, C., & Akilli, H. Flow structure over the yawed nonslender diamond wing. *Aerosp Sci Technol.* **23** (1), 108-119 (2012).
17. Kohlman, D. L., & Wentz, J. W. H. Vortex breakdown on slender sharp-edged wings. *J Aircraft.* **8** (3), 156-161 (1971).
18. Lu, L., & Sick, V. High-speed Particle Image Velocimetry Near Surfaces. *J Vis Exp.* (76), 50559 (2013).
19. Mitchell, A. M., Barberis, D., Molton, P., Dé, J., & lery. Oscillation of Vortex Breakdown Location and Blowing Control of Time-Averaged Location. *AIAA J.* **38** (5), 793-803 (2000).
20. Shen, L., Wen, C.-y., & Chen, H.-A. Asymmetric Flow Control on a Delta Wing with Dielectric Barrier Discharge Actuators. *AIAA J.* **54** (2), 652-658 (2016).
21. Leibovich, S. The Structure of Vortex Breakdown. *Annu Rev Fluid Mech.* **10** (1), 221-246 (1978).
22. Mitchell, A. M., & Molton, P. Vortical Substructures in the Shear Layers Forming Leading-Edge Vortices. *AIAA J.* **40** (8), 1689-1692 (2002).
23. Gad-El-Hak, M., & Blackwelder, R. F. The discrete vortices from a delta wing. *AIAA J.* **23** (6), 961-962 (1985).
24. Zhou, J., Adrian, R. J., Balachandar, S., & Kendall, T. M. Mechanisms for generating coherent packets of hairpin vortices in channel flow. *J. Fluid Mech.* **387** 353-396 (1999).
25. Adrian, R. J., Christensen, K. T., & Liu, Z. C. Analysis and interpretation of instantaneous turbulent velocity fields. *Exp Fluids.* **29** (3), 275-290 (2000).
26. Yoda, M., & Hesselink, L. A three-dimensional visualization technique applied to flow around a delta wing. *Exp. Fluids.* **10** (2-3) (1990).
27. Greenwell, D. I. in *RTO AVT Symposium.* RTO-MP-069(I) Loen, Norway (2001).
28. Furman, A., & Breitsamter, C. Turbulent and unsteady flow characteristics of delta wing vortex systems. *Aerosp Sci Technol.* **24** (1), 32-44 (2013).
29. Wang, C., Gao, Q., Wei, R., Li, T., & Wang, J. 3D flow visualization and tomographic particle image velocimetry for vortex breakdown over a non-slender delta wing. *Exp Fluids.* **57** (6) (2016).

Copyright © 2018 Journal of Visualized Experiments